

Plant cyclotides disrupt epithelial cells in the midgut of lepidopteran larvae

Barbara L. Barbeta*, Alan T. Marshall^{†‡}, Amanda D. Gillon*, David J. Craik[§], and Marilyn A. Anderson*[¶]

Departments of *Biochemistry and [†]Zoology, and [‡]Analytical Electron Microscopy Laboratory, La Trobe University, Melbourne, Victoria 3086, Australia; and [§]Institute for Molecular Bioscience, University of Queensland, Brisbane, Queensland 4072, Australia

Communicated by Adrienne Clarke, University of Melbourne, Victoria, Australia, October 30, 2007 (received for review February 1, 2007)

Several members of the Rubiaceae and Violaceae plant families produce a series of cyclotides or macrocyclic peptides of 28–37 aa with an embedded cystine knot. The cyclic peptide backbone together with the knotted and strongly braced structure confers exceptional chemical and biological stability that has attracted attention for potential pharmaceutical applications. Cyclotides display a diverse range of biological activities, such as uterotonic action, anti-HIV activity, and neurotensin antagonism. In plants, their primary role is probably protection from insect attack. Ingestion of the cyclotide kalata B1 severely retards the growth of larvae from the Lepidopteran species *Helicoverpa armigera*. We examined the gut of these larvae after consumption of kalata B1 by light, scanning, and transmission electron microscopy. We established that kalata B1 induces disruption of the microvilli, blebbing, swelling, and ultimately rupture of the cells of the gut epithelium. The histology of this response is similar to the response of *H. armigera* larvae to the *Bacillus thuringiensis* delta-endotoxin, which is widely used to control these insect pests of crops such as cotton.

circular peptides | insecticidal | kalata B1 | Lepidoptera | microscopy

Cyclotides are a series of cyclic minipeptides of 28–37 aa that are expressed at high levels in the leaves, stems, and roots of several plant species (1, 2). They have an unusual topology based on a cyclic peptide backbone together with a cystine knot in which two disulfide bonds are threaded by a third disulfide bond (2, 3). This structure forces hydrophobic amino acids onto the surface of the molecule, creating a hydrophobic face on the otherwise hydrophilic surface. The cyclotides are thus soluble in both organic and aqueous solvents and are very stable at extremes of pH and temperature (4). The absence of free N and C termini, together with the tightly packed cystine knot, also renders the cyclotides resistant to the activity of proteases (4). The cyclotides are the largest family of circular proteins, although others have been described in bacteria, plants, and animals (5).

Cyclotides were first isolated from the African plant *Oldenlandia affinis*. Two peptides, kalata B1 and B2, were recognized as the active components in a traditional medicine used to accelerate childbirth (6). Additional members of the cyclotide family were subsequently identified in screening studies directed toward discovery of bioactive molecules such as neurotensin antagonists (7), inhibitors of HIV replication (8), and hemolytic agents (9). More than 100 cyclotides have since been isolated from various members of the Rubiaceae, Violaceae, and Cucurbitaceae plant families (10, 11). A single plant may have at least 12 cyclotide genes and produce dozens of different cyclotides (12–14). Although an earlier study reported antimicrobial activity (15), it appears that their predominant activity in plants is insecticidal (13, 16). Jennings *et al.* (13) demonstrated that *Helicoverpa punctigera* failed to develop past the second instar stage when raised on artificial diets containing the cyclotide kalata B1 (13). Similar observations of severe growth retardation were also observed with *Helicoverpa armigera* after ingestion of the kalata B1, B2, and B5 cyclotides (16). Those studies established that the cyclotides did not affect the activity of larval

digestive enzymes such as α -amylase, trypsin, or chymotrypsin, but did not establish whether the growth retardant effect was caused by an antifeedant or toxic effect (13).

In the current study, we describe the effect of the cyclotide kalata B1 on the morphology of midgut epithelial cells of *H. armigera* larvae. Swelling and lysis of the columnar and goblet cells was evident at both light and electron microscopic levels, providing an explanation for the insecticidal activity of cyclotides against lepidopteran pests. The changes in morphology observed resemble the substantial changes to the insect midgut that are induced by the delta-endotoxins from *Bacillus thuringiensis* (17).

Results

The sequence and structure of kalata B1 are illustrated in Fig. 1. The 29-aa peptide is excised from the 11-kDa precursor protein Oak1 (13) and ligation of Gly-1 and Asn-29 results in cyclization, as indicated in Fig. 1. Because of this processing mechanism, it was of interest to compare the insecticidal activity of the corresponding synthetic linear derivative of kalata B1 with that of the natural cyclic molecule. The linear derivative is hereafter referred to as linear B1.

Effects of Kalata B1 on Growth of *H. armigera*. Third-instar larvae were starved for 6 h before they were placed on an artificial diet containing kalata B1 [0.13% (wt/vol) and 0.24% (wt/vol)] or casein as a control. Consumption of diet and production of fecal pellets were monitored. During the 16-h bioassay, individuals within the control group fed continuously, consuming all 330 mg of diet. In contrast, larvae on the kalata B1 diets fed for a short period and moved away from the diet. Fig. 2 shows the mean weight of individuals from each of the three diet groups and the amount of diet remaining at the end of the bioassay and the fecal pellets produced. Control larvae doubled in size over the 16-h bioassay. Larvae on the diet with the highest concentration of kalata B1 [0.24% (wt/vol)] did not grow, consumed very little, and produced few fecal pellets. Larvae exposed to the lower concentration of kalata B1 were only 16% larger than larvae fed on the highest concentration of kalata B1 even though they had consumed about half the diet and produced an intermediate amount of fecal pellets relative to the other two groups.

Effects of Kalata B1 on the Midgut of *H. armigera* Larvae. The diameter of the gut in the control larvae (Fig. 3A) was approximately three times larger than the gut of larvae that had ingested kalata B1 [0.13% (wt/vol) or 0.24% (wt/vol)], reflecting the impact of kalata B1 on larval growth during the 16-h bioassay. Exposure to kalata B1 also led to substantial thickening of the epithelial layer (Fig. 3B and C). In control larvae, this layer consisted of a single layer of columnar and goblet cells. Stem

Author contributions: B.L.B. and M.A.A. designed research; B.L.B. and A.T.M. performed research; D.J.C. contributed new reagents/analytic tools; B.L.B., A.T.M., A.D.G., and M.A.A. analyzed data; and B.L.B., A.D.G., and M.A.A. wrote the paper.

The authors declare no conflict of interest.

[¶]To whom correspondence should be addressed. E-mail: m.anderson@latrobe.edu.au.

© 2008 by The National Academy of Sciences of the USA

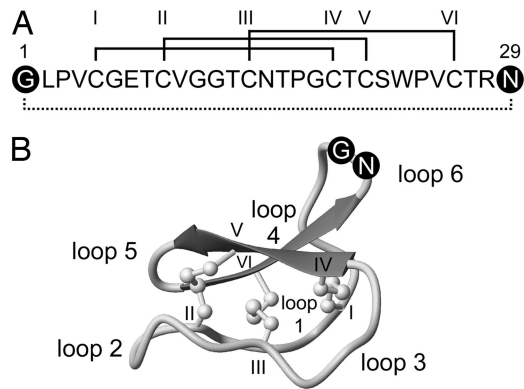


Fig. 1. Sequence and structure of kalata B1. (A) Amino acid sequence of kalata B1 showing disulfide connectivities (roman numerals) and the circular peptide backbone (dotted line). The first and last residues in the mature domain are in black circles (Gly-1 and Asn-29). (B) A ribbon structure of mature kalata B1 (Protein Data Bank ID code 1NB1) (39). The six cysteine residues are labeled with roman numerals, and the six inter-cysteine segments (loops) are numbered 1–6. Loop 6 is completed by the formation of a new peptide bond between Gly-1 and Asn-29 to produce the circular peptide backbone. The acyclic kalata B1 permutant has a break in the peptide bond between Gly-1 and Asn-29.

cells were also evident at the basement membrane, but were relatively sparse (Fig. 3D). The cavity of the goblet cells spanned most of the width of the epithelial layer. After ingestion of diet containing 0.13% (wt/vol) kalata B1, the epithelial layer appeared two to three times thicker (Fig. 3B). This size increase was caused in part by elongation of the cells, but resulted mainly from substantial blebbing of cell fragments into the gut lumen. Beneath the layer of cell fragments the epithelial layer appeared intact. There was also a slight increase in the number of stem cells.

A more severe effect was observed at the higher concentration of kalata B1 (Fig. 3C and F). The single layer of epithelial cells was no longer evident. The columnar cells were swollen and had lysed and released granular material onto the epithelial surface and into the gut lumen. The brush border was disrupted and the peritrophic membrane had lost normal morphology. The number of stem cells at the basement membrane had increased substantially, displacing the damaged columnar and goblet cells.

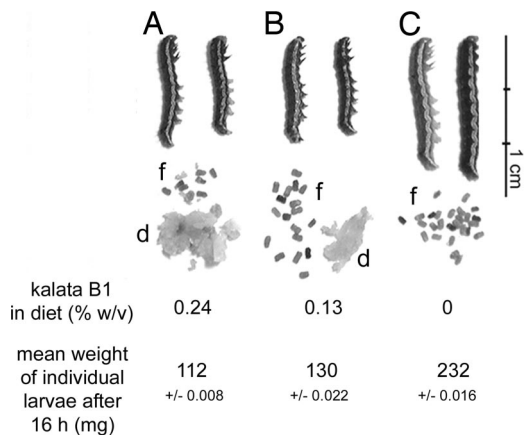


Fig. 2. The appearance and mean average weight of third-instar larvae after 16 h on control diet (C) or diets containing 0.24% (wt/vol) (A) or 0.13% (wt/vol) (B) kalata B1. Diet (d) not consumed after 16 h and the amount of fecal pellets (f) produced by an individual larvae from each group are also shown. As the concentration of kalata B1 increased less diet was consumed and fewer fecal pellets were produced.

At both concentrations of cyclotide, the damage was more obvious in the anterior than the posterior region of the midgut (data not shown).

Electron Microscopic Analysis. Scanning electron micrographs of the surface of the epithelial layer in control larvae (Fig. 4A) showed that it was relatively flat compared with the balloon-like appearance of epithelial cells that had been exposed to kalata B1 (Fig. 4B). An intact peritrophic membrane and the brush border (Fig. 4C) were evident in freeze-fractured faces of the midgut of the control fed larvae. In contrast, in the kalata B1-fed individuals the gut epithelial layer was twice as thick as the control individuals and the surface of the cells was covered with granular material. The brush border was not evident on the surface of the swollen cells but was present on columnar cells that had not expanded. These cells may not be affected by the cyclotide. Alternatively, the cells may have developed after the larvae had stopped eating. The peritrophic membrane was not detected (Fig. 4D).

Transmission electron microscopy was used to investigate the effect of cyclotides on the appearance of cell membranes and cellular organelles. In control larvae, the anterior midgut epithelium consisted of cuboidal columnar cells, goblet cells, and stem cells (Fig. 5A). The epithelium was separated from the gut lumen by a well defined peritrophic membrane. The apical region of the columnar cells contained numerous mitochondria, lipid droplets, and extensive glycogen deposits (Fig. 5B). At the basal side of the absorptive cells, the basal membrane formed short sparse infoldings (Fig. 5C). In contrast, in the anterior midgut epithelium of kalata B1-treated larvae (Fig. 5D–F) the cytoplasm of the columnar cells appeared denser than in control larvae, indicating a higher intracellular osmotic concentration and consequently greater shrinkage during fixation. The peritrophic matrix was poorly defined and the apical region of the absorptive cells was characteristically swollen with a reduced complement of apical microvilli (Fig. 5E). The cells had few mitochondria and few glycogen deposits relative to control cells. Unlike control cells, the basal membrane was highly infolded (Fig. 5F).

Effects of Linear Kalata B1 on the Midgut of *H. armigera* Larvae. To determine whether the cyclic backbone is essential for insecticidal activity, we synthesized kalata B1 protein with a break in the peptide backbone in loop 6 between Gly-1 and Asn-29 but with disulfide bonds intact (Fig. 1) and repeated the 16-h bioassay. Larvae consumed all of the diet containing linear kalata B1, and growth was equivalent to that of larvae fed the control diet. Light microscopy of the gut epithelium revealed some sloughing of cell fragments into the lumen but no swelling, cell lysis, or proliferation of stem cells (Fig. 6).

Discussion

In this study, we show that ingestion of cyclotides causes marked changes in the midgut of lepidopteran pests and provide an explanation for the observed insecticidal activity of cyclotides. At the highest concentration of cyclotide [0.24% (wt/vol)] very little diet was consumed but the larvae did not die, suggesting the cyclotide is not highly toxic and that the failure to grow was probably caused by the lack of nutrient intake. At the lower concentration of cyclotide, up to half the diet was consumed, but larval growth was poor relative to the controls, indicating nutrient uptake was still impaired. We then asked whether the midgut had been damaged; it has a crucial role in digestion and absorption and is often the target for insecticidal proteins.

The damage we observed, such as blebbing of the midgut epithelial cells, cell swelling, and lysis, was similar to the changes in gut morphology induced by the most effective insecticidal proteins from bacterial species, including the δ -endotoxins (17)

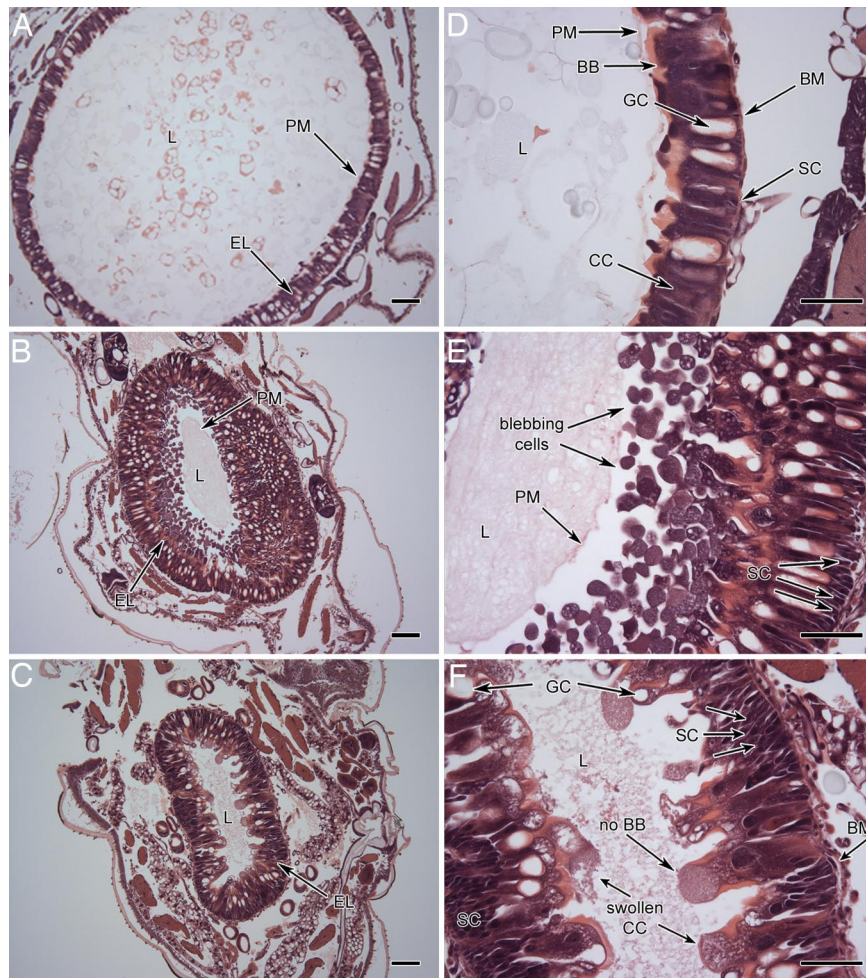


Fig. 3. Light microscopy of the anterior midgut third-instar larvae fed for 16 h on control and kalata B1 diets. Columnar cells (CC), goblet cells (GC), brush border (BB) of the columnar cells, lumen (L), peritrophic membrane (PM), and epithelial layer (EL) are as labeled. Stem cells (SC) are located along the basement membrane (BM) between columnar and goblet cells. (A and D) The midgut epithelium of third-instar larva after ingestion of control diet (16 h). (B and E) Kalata B1-fed [0.13% (wt/vol)] larva. The diameter of the gut is smaller than the gut in control larvae. The epithelial layer appears thicker because of blebbing of epithelial cells into the gut lumen. (C and F) Kalata B1-fed [0.24% (wt/vol)] larva. The width of the cell layer was much greater than the width of that in the control larvae. CCs were elongated and swollen and some had burst releasing granular material into the lumen. The loss of brush border at the apex of columnar cells is indicated by arrows. The peritrophic membrane was not visible. At the basement membrane the number of stem cells had increased significantly. (Scale bars: A–D, 100 μ m; E and F, 50 μ m.)

and Vip3A (18) from *B. thuringiensis* and toxin complex A from *Photorhabdus luminescens* (19). Similar effects have also been reported for cholesterol oxidase (20).

The larval response to cyclotide damage to midgut cells was proliferation of the basal stem cells. Rapid division of stem cells is normally restricted to the period of the larval moult, but is also responsible for cell replacement during repair (17, 21). All of the larvae examined in this study were at the midmoult stage; hence, the stem cell proliferation observed was a reflection of the damage caused by the cyclotides. The proliferation of stem cells also indicates that the larvae would probably recover if they were transferred to a cyclotide-free diet. Those studies were undertaken and confirmed this hypothesis (data not shown).

Light microscopy indicated that the microvilli on the columnar cells were disrupted after cyclotide ingestion. This disruption was more obvious in the scanning and transmission electron micrographs. The damage to the absorptive surface together with the occlusion of the epithelial layer by the granular material released from the lysed cells would explain the poor uptake of nutrients by the cyclotide-fed larvae.

Nutrient uptake would also be negatively affected by damage to the peritrophic membrane, which has a key role in digestion

and also functions to protect the epithelial cells from damage by the food bolus (22). The peritrophic membrane was either damaged or absent in the cyclotide-fed larvae. This damage may have been caused by the swelling and fragmenting cells. However, a direct effect of cyclotides on the peritrophic membrane cannot be discounted because it is a known target for some insecticidal molecules (23, 24).

It is most likely that cyclotides disrupt the plasma membrane of the epithelial cells, forming holes or pores that lead to cell swelling and lysis. This hypothesis is consistent with the observation that cyclotide ingestion induces a midgut morphology that closely resembles the morphology produced by the Cry toxins, Vip3A and cholesterol oxidase (20). The Cry toxins and Vip3A are much larger (>60 kDa) than the 3-kDa cyclotides. They bind to specific receptors on the midgut membrane and assemble into oligomers that form distinct pores in the membrane. Pore formation can occur in artificial bilayers in the absence of the receptor, but it is slower and requires more protein than pore formation in the gut epithelial membrane (25, 26). Specific receptors for cyclotide binding have not been reported, but we have demonstrated that cyclotides bind directly to lipids, pre-

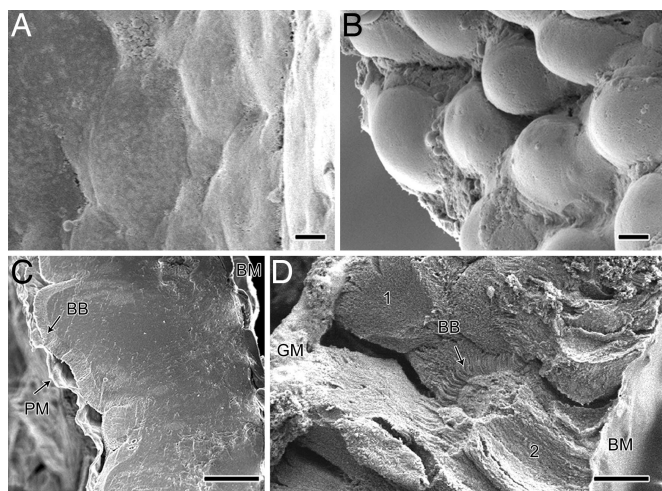


Fig. 4. Scanning electron micrographs of anterior midgut epithelia after ingestion of control (A and C) and kalata B1 [0.24% (wt/vol)] (B and D) diets. The luminal surface is shown in A and B, and a transverse section from freeze fracture is shown in C and D. Gut from kalata B1-fed larvae had columnar cells that were swollen and protruding into the lumen and granular material (GM) was entangled with the peritrophic membrane (D). Brush border (BB), basement membrane (BM), a swollen cell (labeled 1), a nonswollen columnar cell (labeled 2), and peritrophic membrane (PM) are indicated. (Scale bars: 10 μm .)

sumably via the hydrophobic patch that is exposed on their surface (27).

Such a binding mode was proposed recently based on spin-label studies of kalata B1 binding to dodecylphosphocholine

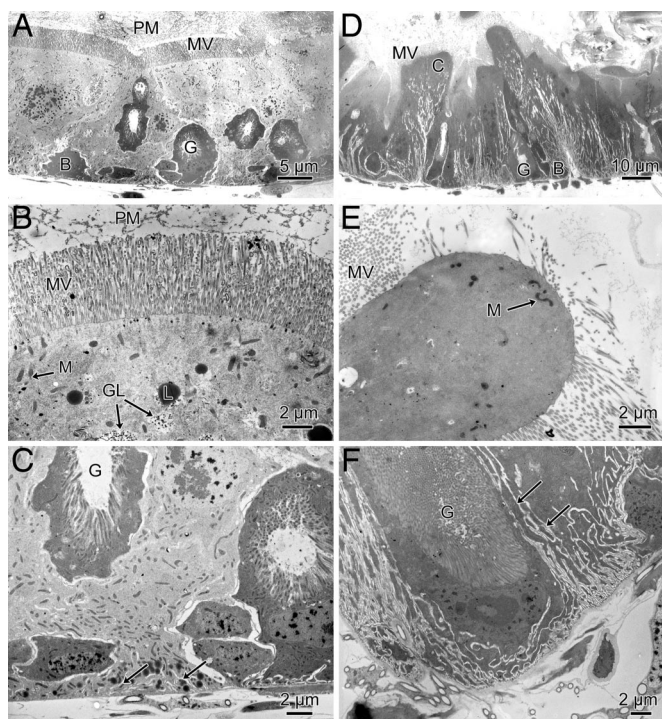


Fig. 5. Transmission electron microscopy of the anterior midgut epithelia of midsecond-instar larvae fed control diet (A–C) and diet supplemented with kalata B1 [0.24% (wt/vol)] (D–F). A and D show a cross section of the complete epithelium comprising columnar cells (C) and goblet cells (G). B and E show the apical regions of columnar cells with apical microvilli (MV), mitochondria (M), lipid droplets (L), and glycogen deposits (GL). The peritrophic membrane is evident in control larvae (B). C and F show the basal region of columnar cells with arrows indicating basal infoldings. (Scale bars: 2 μm .)

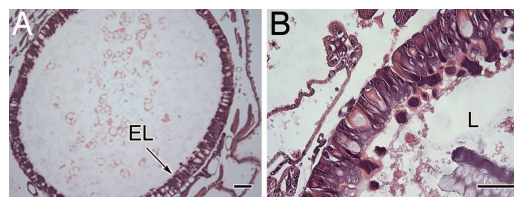


Fig. 6. The effects of linear kalata B1 protein on the midgut of third-instar larvae after 16 h. (A) Control tissue. (B) Linear kalata B1 [0.24% (wt/vol)] produced increased shedding of cells from the epithelial layer (EL) into the lumen (L). No other damage was observed. (Scale bars: A, 100 μm ; B, 50 μm .)

micelles (28). Surface plasmon resonance studies indicate that cyclotides bind more strongly to phosphatidylethanolamine-containing lipids than a range of other lipid mixtures (27), indicating selectivity for some membranes over others and perhaps explaining the specific effects on the insect midgut cells. We (29) have also shown that some cyclotides assemble into tetramers and octamers in solution and thus potentially could assemble into pores in membranes. Further evidence for their ability to disrupt membranes is seen from their hemolytic activity (30) and their cytotoxic effect on a human lymphoma cell line (31).

Previous studies have revealed that cyclotide activity can be lost after breakage of the circular peptide backbone. Hemolytic activity was lost when the kalata B1 backbone was broken in loops 2, 3, 5, or 6 despite native folds (30, 32), and anti-HIV activity was lost after a break in loop 6 (33). Because a break in the peptide backbone was sufficient to neutralize kalata B1 activity in this study, we suggest that the circular backbone is important in maintaining framework stability, which, in turn, is essential for insecticidal activity.

Most plant insecticidal proteins target digestive enzymes (34, 35) or the chitin in the peritrophic matrix (36). Although they do retard insect growth and impart some damage to the membrane, they rarely lead to the damage that we have observed with the cyclotides and generally do not stop the insect from feeding.

The African plant *O. affinis* produces 2 g of cyclotides/kg of fresh weight (37), which is comparable with the levels used in the bioassays described here and thus is sufficient to protect the plants from damage by lepidopteran pests.

Experimental Procedures

Bioassays with Artificial Diets. *H. armigera* larvae were raised on an artificial diet based on haricot beans (13). Wheat germ was suspended in water and boiled for 20 min to inactivate the wheat germ lectin before incorporation into the diet. Larvae were raised from neonates to the midsecond (electron microscopy) and early-third (light microscopy) instar stage of development, before they were starved for 6 h and transferred to test diets supplemented with kalata B1 peptide [0.13% (wt/vol) or 0.24% (wt/vol)] or linear kalata B1 [0.24% (wt/vol)]. The cyclic kalata B1 and linear B1 (Fig. 1) were prepared as described (32). The control diet contained casein in place of the inhibitor. Each larva was placed in a clean 1.5-ml microfuge tube containing 330 mg of diet and was maintained at $25 \pm 1^\circ\text{C}$, 16:8 h (light/dark). After 16 h, the larvae were weighed, and the amount of fecal pellets produced and diet remaining was recorded. Three larvae were used for each diet. The bioassay was performed three times.

Light Microscopy. The larvae were removed from the diet and placed on ice for 20 min to slow activity before they were killed with ethyl acetate. Formal saline or Bouin's fluid was injected into the anterior and posterior ends with a 27-gauge needle. The larvae were then immersed in fixative and sent to Austin Health for paraffin embedding, sectioning, and hematoxylin and eosin staining. The sections were viewed with an Olympus BX41 microscope, and images were captured with QCapture 2.86.6 software (Media Cybernetics).

Sample Preparation for Electron Microscopy. The gut was excised from the larvae and placed in fixative [2.5% (wt/vol) glutaraldehyde, 0.2 M sodium

phosphate buffer (pH 7.2), osmolarity 333 mOsmols·kg⁻¹] before transfer to fresh fixative and storage at 4°C. The gut was then rinsed (3 × 5 min) in 0.2 M phosphate buffer and prepared for scanning or transmission electron microscopy.

Scanning Electron Microscopy. The gut was placed in 2% (wt/vol) OsO₄ in 0.2 M phosphate buffer for 2 h and rinsed in wash buffer (10 × 15 min) before immersion in fresh 1% (wt/vol) thiocarbonylhydrazide for 10 min followed by 10- to 15-min rinses in distilled water. The gut was postfixed in 2% (wt/vol) OsO₄ for 30 min and rinsed in distilled water before dehydration in an ethanol series (70%, 95%, and 100%). The dehydrated samples were freeze-fractured in liquid nitrogen and dehydrated further by using 100% acetone followed by 100% hexamethyldisilane. The tissue was platinum-coated (2 nm) by using a

Polaron SC7640 Sputter Coater and viewed with a JOEL JSM-6340 field emission scanning electron microscope.

Transmission Electron Microscopy. The gut was postfixed in 2% (wt/vol) OsO₄ in 0.2 M phosphate buffer, dehydrated in an ethanol series, and embedded in Araldite 502 resin (ProSciTech). Ultrathin transverse sections of the anterior midgut were stained with uranyl acetate and Sato's lead stain (38) before they were viewed at 80 kV in a JOEL 1200EX transmission electron microscope.

ACKNOWLEDGMENTS. We thank Simon Eade at Austin Health for preparation of paraffin sections. This work was supported by a grant from the Australian Research Council. D.J.C. is an Australian Research Council Professional Fellow.

1. Craik DJ, Daly NL, Bond T, Waine C (1999) *J Mol Biol* 294:1327–1336.
2. Craik DJ, Cemazar M, Wang CK, Daly NL (2006) *Biopolymers* 84:250–266.
3. Saether O, et al. (1995) *Biochemistry* 34:4147–4158.
4. Colgrave ML, Craik DJ (2004) *Biochemistry* 43:5965–5975.
5. Craik DJ (2006) *Science* 311:1563–1564.
6. Gran L (1970) *Meddelelser Norsk Farmaceutisk Selskap* 32:173–180.
7. Witherup KM, et al. (1994) *J Nat Prod* 57:1619–1625.
8. Gustafson KR, McKee TC, Bokesch HR (2004) *Curr Protein Pept Sci* 5:331–340.
9. Schöpke T, Hasan AMI, Kraft R, Otto A, Hiller K (1993) *Scientia Pharmaceutica* 61:145–153.
10. Craik DJ, Daly NL, Mulvenna J, Plan MR, Trabi M (2004) *Curr Protein Pept Sci* 5:297–315.
11. Simonsen SM, et al. (2005) *Plant Cell* 17:3176–3189.
12. Dutton JL, et al. (2004) *J Biol Chem* 279:46858–46867.
13. Jennings C, West J, Waine C, Craik D, Anderson M (2001) *Proc Natl Acad Sci USA* 98:10614–10619.
14. Mulvenna JP, Sando L, Craik DJ (2005) *Structure (London)* 13:691–701.
15. Tam JP, Lu YA, Yang JL, Chiu KW (1999) *Proc Natl Acad Sci USA* 96:8913–8918.
16. Jennings CV, et al. (2005) *Biochemistry* 44:851–860.
17. Spies AG, Spence KD (1985) *Tissue Cell* 17:379–394.
18. Yu CG, Mullins MA, Warren GW, Koziel MG, Estruch JJ (1997) *Appl Environ Microbiol* 63:532–536.
19. Blackburn M, Golubeva E, Bowen D, French-Constant RH (1998) *Appl Environ Microbiol* 64:3036–3041.
20. Purcell JP, et al. (1993) *Biochem Biophys Res Commun* 196:1406–1413.
21. Loeb MJ, Martin PA, Hakim RS, Goto S, Takeda M (2001) *J Insect Physiol* 47:599–606.
22. Ryerse, JS., Purcell, JP., Sammons, RD., Lavrik, PB (1992) *Tissue Cell* 24:751–771.
23. Hopkins TL, Harper MS (2001) *Arch Insect Biochem Physiol* 47:100–109.
24. Pechan T, Cohen A, Williams WP, Luthe DS (2002) *Proc Natl Acad Sci USA* 99:13319–13323.
25. Puntheeranurak T, Stroh C, Zhu R, Angsuthanasombat C, Hinterdorfer P (2005) *Ultra-microscopy* 105:115–124.
26. Vie V, et al. (2001) *J Membr Biol* 180:195–203.
27. Kamimori H, Hall K, Craik DJ, Aguilar MI (2005) *Anal Biochem* 337:149–153.
28. Shenkarev ZO, et al. (2006) *FEBS J* 273:2658–2672.
29. Nourse A, Trabi M, Daly NL, Craik DJ (2004) *J Biol Chem* 279:562–570.
30. Barry DG, Daly NL, Clark RJ, Sando L, Craik DJ (2003) *Biochemistry* 42:6688–6695.
31. Svargard E, et al. U (2007) *J Nat Prod* 70:643–647.
32. Daly NL, Craik DJ (2000) *J Biol Chem* 275:19068–19075.
33. Daly NL, Gustafson KR, Craik DJ (2004) *FEBS Lett* 574:69–72.
34. Morton RL, et al. (2000) *Proc Natl Acad Sci USA* 97:3820–3825.
35. Carlini CR, Grossi-de-Sa MF (2002) *Toxicol* 40:1515–1539.
36. Gongora CE, Wang S, Barbehenn RV, Broadway RM (2001) *Entomol Exp Appl* 99:193–204.
37. Gran L (1973) *Lloydia* 36:174–178.
38. Sato T (1968) *J Electron Microsc* 17:158–159.
39. Rosengren KJ, Daly NL, Plan MR, Waine C, Craik DJ (2003) *J Biol Chem* 278:8606–8616.